Solvent Effect on Electrochemical CO_2 Reduction Reaction on Nanostructured Copper Electrodes

Deacon-Price, C.; da Silva, A.H.M.; Santana, C.S.; Koper, M.T.M.; Garcia, A.C.

DOI
10.1021/acs.jpcc.3c03257

Publication date
2023

Document Version
Final published version

Published in
The Journal of Physical Chemistry. C

THE JOURNAL OF PHYSICAL CHEMISTRY C
A JOURNAL OF THE AMERICAN CHEMICAL SOCIETY

pubs.acs.org/JPCC

Article

Solvent Effect on Electrochemical CO_2 Reduction Reaction on Nanostructured Copper Electrodes

Connor Deacon-Price, Alisson H. M. da Silva, Cássia S. Santana, Marc T. M. Koper, and Amanda C. Garcia*

Cite This: *J. Phys. Chem. C* 2023, 127, 14518–14527

Read Online

ACCESS | Metrics & More | Article Recommendations | Supporting Information

ABSTRACT: The electrochemical reduction of CO_2 (CO_2RR) is a sustainable alternative for producing fuels and chemicals, although the production of highly desired hydrocarbons is still a challenge due to the higher overpotential requirement in combination with the competitive hydrogen evolution reaction (HER). Tailoring the electrolyte composition is a possible strategy to favor the CO_2RR over the HER. In this work we studied the solvent effect on the CO_2RR on a nanostructured Cu electrode in acetonitrile solvent with different amounts of water. Similar to what has been observed for aqueous media, our online gas chromatography results showed that CO_2RR in acetonitrile solvent is also structure-dependent, since nanocube-covered copper (CuNC) was the only surface (in comparison to polycrystalline Cu) capable of producing a detectable amount of ethylene (10% FE), provided there is enough water present in the electrolyte (>500 mM). In situ Fourier Transform Infrared (FTIR) spectroscopy showed that in acetonitrile solvent the presence of CO_2 strongly inhibits HER by driving away water from the interface. CO is by far the main product of CO_2RR in acetonitrile (>85% Faradaic efficiency), but adsorbed CO is not detected. This suggests that in acetonitrile media CO adsorption is inhibited compared to aqueous media. Remarkably, the addition of water to acetonitrile has little quantitative and almost no qualitative effect on the activity and selectivity of the CO_2RR. This indicates that water is not strongly involved in the rate-determining step of the CO_2RR in acetonitrile. Only at the highest water concentrations and at the CuNC surface, the CO coverage becomes high enough that a small amount of C_{2+} product is formed.

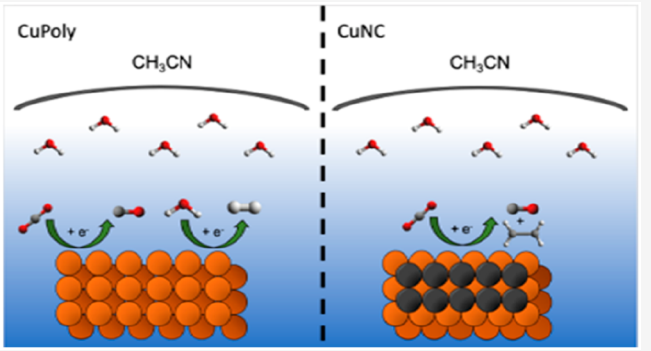

1. INTRODUCTION

The electrochemical reduction of carbon dioxide (CO_2RR) offers a sustainable pathway to address some of the future energy needs by converting waste into fuels and chemicals without relying on fossil fuels derivatives.[1−4] Although electrochemistry has the promising ability to operate at room temperature and pressure,[5] CO_2RR is still hampered by low energy efficiency related to the high overpotential required, especially in the conversion of CO_2 to highly reduced C_{2+} products,[6] and the poor long-term stability of electrocatalysts.[7] Furthermore, because most CO_2 electrolyses are performed in aqueous media, hydrogen evolution reaction (HER) occurs simultaneously with CO_2RR, limiting the Faradaic efficiency (FE) toward CO_2RR products.[8,9]

Tailoring the catalyst surface is the most common way to steer activity and selectivity to favor CO_2RR over HER.[10,11] Many recent studies, however, have showed the importance of the electrolyte composition on the reaction rate of CO_2 reduction and H_2 evolution.[12−15] Recently, Monteiro et al.[16] showed that the electrochemical reduction of CO_2 to CO on gold, copper, and silver electrodes requires the presence of a cation to coordinate and, hence, to stabilize the first electron-transfer intermediate $CO_2^{\bullet-}$. Nevertheless, an intermediate cation concentration is preferable, as cations also promote the concomitant water and bicarbonate reduction, favoring hydrogen evolution.[2,12,15,17−20] Therefore, if water is the main proton donor, the activity for the hydrogen evolution reaction can be altered by changing the cation and its interfacial concentration.

An alternative strategy to promote CO_2RR over HER is to replace water with an organic solvent, such as acetonitrile,[21] dimethylformamide,[22] or methanol.[23] These solvents have lower proton and/or water availability, which should lower the hydrogen evolution rate. Previous studies by Amatore and Saveánt[22] showed that CO_2RR in dry dimethylformamide

Received: May 17, 2023
Revised: June 27, 2023
Published: July 12, 2023

proceeds through three competing pathways: (1) oxalate formation through self-coupling of the $CO_2^{\bullet-}$ anion radicals, (2) CO and CO_3^{2-} formation via oxygen−carbon coupling of $CO_2^{\bullet-}$ with CO_2, and (3) formate formation through protonation of $CO_2^{\bullet-}$ by residual water, followed by a homogeneous electron transfer from $CO_2^{\bullet-}$. On the other hand, Figueiredo et al.,[21] using a copper electrode in acetonitrile containing small amounts of water, found that the main products from CO_2RR are carbonate, bicarbonate, and CO. However, the formation of CO and carbonate was suggested to be decoupled from each other by the influence of residual water. The formation of carbonate and bicarbonate species appears to be the result of a solution-phase reaction of CO_2 with electrochemically generated OH^- from the water reduction.

Considering the key role of the solvent composition on CO_2 reduction, it would be attractive to understand the mechanism of the CO_2RR toward hydrocarbon products in acetonitrile solvent and how the presence of water influences the product distribution and the competition between the CO_2RR and HER.

Much of the work present in the literature attempting to understand the CO_2RR mechanism in aqueous electrolytes has been based on theoretical and experimental studies with well-oriented Cu single crystal surfaces. These studies showed that Cu(100) surfaces[24−28] are particularly interesting because of their high selectivity to C_{2+} products, like ethylene and ethanol[21,24,29,30] in comparison to Cu(111) surfaces, which are more selective for the generation of CH_4.[24,25,27,28] The higher selectivity of Cu(100) toward hydrocarbons compared to Cu(111) was previously related to the CO-binding energy on the electrode surface,[25,31−33] which is considered to be crucial for the OC−CO dimerization and, therefore, to make hydrocarbon products.[27,34−36] More recently, studies using ultrahigh vacuum preparation and spectroscopic characterization,[29] however, showed that copper single crystals with clean, flat, and atomically ordered surfaces do not exhibit high selectivity to hydrocarbons, instead favoring hydrogen evolution. Only the introduction of defects and roughness, for example, by electropolishing or O_2-plasma treatment, shifts the selectivity toward hydrocarbons. This change in mechanism is due to the stronger CO-binding strength on the defected surface, which is more predominant on Cu_2O species that originated on the surface of Cu(100) after the electrochemical pretreatment.

In this work, we prepared copper oxide-derived (Cu_xO) electrodes with different morphologies through electro-oxidative/reductive cycles and tested their activity and selectivity for the CO_2RR in acetonitrile solution. Through a combination of electrochemical measurements with online gas chromatography (GC) and in situ Fourier Transform Infrared (FTIR) spectroscopy, we studied the electrochemical reduction of CO_2 in acetonitrile solvent in the presence of different amounts of water on Cu nanocubes (CuNC) and polycrystalline Cu (CuPoly) electrodes. Our results show that, in acetonitrile, CO is by far the dominant product, regardless of the water concentration in the electrolyte. This shows that the competition between the CO_2RR and HER in acetonitrile is very different from the situation in aqueous media. However, similar to aqueous media,[27,37] CO_2RR selectivity toward C_{2+} products in acetonitrile is dependent on the electrode structure and electrolyte composition. CuNC is the only surface capable of producing a detectable amount of ethylene (10% FE), provided there is enough water present in the electrolyte (>500 mM).

2. MATERIALS AND METHODS

2.1. Cleaning and Sample Preparation. All water used in this work (resistivity >18.2 MΩ·cm, TOC < 5 ppb) was purified with a Millipore Milli-Q system. All glassware was cleaned from organic contamination by soaking overnight in an aqueous solution of 1 g L^{-1} of $KMnO_4$ (Fluka, ACS reagent) and 0.5 M KOH (Sigma-Aldrich, ACS reagent). Before experiments, this solution was drained, and residual MnO_4^- was decomposed by immersing the glassware in dilute piranha solution (3:1 v/v mix of H_2SO_4 (Sigma-Aldrich, 95−98%)/H_2O_2 (Sigma-Aldrich, 30% w/w)). It was subsequently drained, and all the glassware was boiled in water at least three times to remove inorganic contaminants.

$KHCO_3$ (Sigma-Aldrich, 99.95%), KCl (Sigma-Aldrich, >99%), $HClO_4$ (Sigma-Aldrich, 60%), CH_3CN (Biosolve, 99.9%), and $C_8H_{20}ClN$ (TEACl; ThermoFisher Scientific, 99%) were used as received. CO_2 (Linde, 4.5 purity) and Ar (Linde, 6.0 purity) gases were used to saturate and deaerate the electrolyte solution, respectively.

To ensure that the solvent was as water-free as possible, prior to the experiments, acetonitrile was dried over 3 Å molecular sieves, which had been previously stored at 130 °C. Molecular sieves were first added to a Schlenk tube, which was then flame-dried under vacuum to remove water vapor. A positive pressure of N_2 was applied to the vessel in which acetonitrile was stored. The solvent was then stored under N_2 for a minimum of 24 h before use. Karl Fischer titration showed 1.6 mM (±0.5 mM) H_2O content before use.

2.2. Electrochemical Measurements. Electrochemical measurements were carried out in a single-compartment three-electrode cell with a MultiAutoLab M101 Potentiostat (Metrohm). A polycrystalline Cu disk (CuPoly − ϕ 5 mm) or Cu_xO was used as the working electrode0 (WE). Prior to experiments, the CuPoly disk was polished with a 5.0 μm diamond suspension (Buehler), then rinsed with ultrapure water, followed by sonication in ultrapure water. Next, the electrode was electropolished in a 66% H_3PO_4 (Fisher Scientific, 85%) aqueous solution. A Pt wire was used as the counter electrode (CE) and $Ag/AgCl/KCl_{sat}$ or commercial leak-free Ag/Ag^+ (Alvatek) was used as the reference electrode (RE) in aqueous and organic solvents, respectively. Prior to experiments, we tested the possibility of shifting the potential of the reference Ag/Ag^+ electrode due to the addition of H_2O or saturation with CO_2 by adding the ferrocene/ferrocenium (Fc/Fc^+) redox couple in solution. As shown in Figure S1, no shift was observed.

All potentials measured against the $Ag/AgCl/KCl_{sat}$ electrode were converted to their reversible hydrogen electrode (RHE) values according to eq 1:[12]

$$E_{RHE} = E_{Ag/AgCl(KClsat)} + E^{\circ}_{Ag/AgCl(KClsat)} + 0.059 \times pH \quad (1)$$

All the potential values (E) were corrected for ohmic drop according to eq 2:[14]

$$E_{corrected} = E - [(i \times R_u) \times 85\%] \quad (2)$$

where R_u is the uncompensated resistance measured (ca. 400 Ω in organic solvent). Electrolysis measurements were carried out at −2.0 V versus Ag/Ag^+. The experiments were performed using a homemade two compartment (H-type) electro-

https://doi.org/10.1021/acs.jpcc.3c03257
J. Phys. Chem. C 2023, 127, 14518−14527

chemical cell.[38] An anionic exchange membrane (AHO, AGC Inc.) was used to separate the cathodic and anodic compartments, which were filled with 10 mL of 0.1 M TEACl in MeCN solvent. In the cathodic compartment, CO_2 was continuously bubbled at a fixed flow rate of 15 mL min^{-1} from directly below the WE to avoid mass transport limitations. Different amounts of ultrapure water were added (10, 100, 500, and 1000 mM) into the acetonitrile electrolyte to assess the effect of the proton donor content. A dimensionally stable anode (DSA, Magneto) counter electrode (CE) and a commercial leak-free Ag/Ag^+ (Alvatek) reference electrode (RE) were used for all electrolysis experiments. Water concentrations were measured using a Karl Fischer titration, finding no significant change before and after bubbling of CO_2 into the electrolyte. The potential of the working electrode was controlled by a Bio-Logic potentiostat/galvanostat/EIS (SP-300). Gaseous products were analyzed online using a Shimadzu 2014 gas chromatograph (GC) with two detectors (one TCD and one FID). The analyte was separated before analysis by FID via an RTX-1 column and for TCD via a Shincarbon column. The column temperature was held at 40 °C for 3 min before being increased to 130 °C at a heating rate of 150 °C min^{-1}. Liquid products were measured by high performance liquid chromatography (Prominence HPLC, Shimadzu). A 5 mM H_2SO_4 solution was used as the eluent, separating the analyte over an Aminex HPX-87H (Biorad) column. Flow rate was maintained at 0.6 mL min^{-1} at a column temperature of 45 °C.

2.3. In Situ Fourier Transform Infrared Spectroscopy. To provide information about the surface-adsorbed intermediates and products of the electrochemical reduction of carbon dioxide, in situ FTIR spectra were collected. The FTIR instrument was a Bruker Vertex 80 V IR spectrometer equipped with a liquid nitrogen cooled detector. In situ FTIR experiments were performed in a three electrode spectro-electrochemical cell with a CaF_2 prism attached to the bottom of the cell. Details concerning the cell are described in the literature.[39] FTIR spectra were obtained in the wavenumber range between 4000 and 900 cm^{-1}. Spectra were collected in 0.1 V steps from −1.0 to −2.5 V vs RHE under an argon or CO_2 atmosphere. They were computed from the average of 100 interferograms with the spectral resolution set to 8 cm^{-1}. Spectra are presented as reflectance, according to $A = -\log(R/R_0)$, where R and R_0 are the reflectances corresponding to the single beam spectra obtained at the sample and reference potentials, respectively. In these difference spectra, negative bands (pointing down) correspond to the species that were present on or near the electrode surface at the reference potential and that are "consumed" at the sample potential. Positive bands (pointing up) correspond to the formation of species at the sample potential. All the spectro-electrochemical experiments were performed at room temperature, with Ag/Ag^+ and platinum coils used as reference and counter electrodes, respectively.

2.4. Cu_xO-Derived Nanoparticle Synthesis. Shape-controlled nanoparticle (NP) synthesis was performed via the procedure previously described by Roberts et al.[40] A CuPoly plate (WE) was placed in a three-electrode cell (Pt wire, CE; $Ag/AgCl/KCl_{sat.}$, RE) and then subjected to four oxidation−reduction potential cycles. The electrodes were directly submerged in an aqueous electrolyte solution of 0.1 M $KHCO_3$ solution +4 mM KCl purged with CO_2 to maintain a pH of 6.8.[40] Potentials were cycled from 0.0 V to E_{upper} to −1.2 V versus RHE, where E_{upper} = 0.7, 0.9, or 1.1 V versus RHE, at a scan rate of 5 mV s^{-1}.[40]

The relative electrochemically active surface area (ECSA) of the different copper electrodes were determined by the procedure previously described by Kanan et al.[30,41,42] Argon was bubbled through a 0.1 M $HClO_4$ solution in a three-electrode cell configuration for 20 min to remove all of the dissolved oxygen. To prevent the redissolution of ambient oxygen, a constant flow of Ar was maintained over the solution. Cyclic voltammetry (CV) was performed in the double layer (DL) region, corresponding to a potential range of 0.00 V to −0.12 V vs RHE. After repeating the measurements over six different scan rates (10, 20, 40, 60, 80, and 100 mV s^{-1}), the DL capacitance was extracted from the slope of the linear plot of DL current against scan rate. The positive current was measured at −0.05 V, where no electrochemical activity was found to take place. The roughness factor was then calculated, since the DL capacitance value in the DL region is expected to be proportional to the electrochemically active surface area. By comparison with CuPoly, the RF of the CuNPs can be defined by normalizing the measured capacitances with respect to that of CuPoly. CuPoly is set as reference, which is defined as RF = 1.

For each experimental condition, we used freshly prepared electrodes, with their structures being verified in 0.1 M NaOH before their use.

2.5. Physico-Chemical Characterization. The morphology of the synthesized Cu_xO-based nanoparticles was analyzed by using a Scanning Electron Microscopy (SEM) technique Apreo SEM (ThermoFisher Scientific) with an acceleration voltage of 15 kV and an electron beam current of 0.4 nA.

3. RESULTS

3.1. Physical and Electrochemical Characterization of Oxide-Derived Copper Electrodes. SEM images revealed that the electrochemical oxidation−reduction treatment of polycrystalline Cu (CuPoly) in the Cl^- solution results in different nanostructures, as shown in Figure 1, in agreement with the literature.[40,43] CuPoly (Figure 1A) is included for comparison, and the surface of which remains featureless at the nanoscale level. By sweeping the electrode potential from 0.0 to 0.7 V versus RHE, nanoparticles with the shape of irregular spheres of ∼50 nm were formed (CuNS, Figure 1B), whereas by sweeping the potential up to 0.9 and 1.1 V, irregular

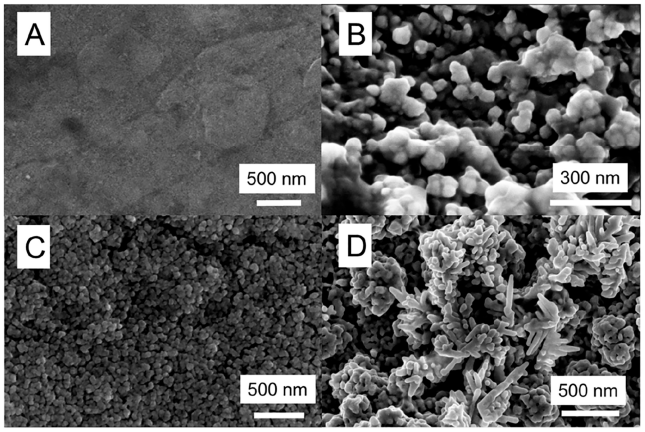

Figure 1. Scanning electron microscopy images of CuPoly(A), CuNS (B), CuNC (C), and CuND (D) oxide-derived materials.

https://doi.org/10.1021/acs.jpcc.3c03257
J. Phys. Chem. C 2023, 127, 14518−14527

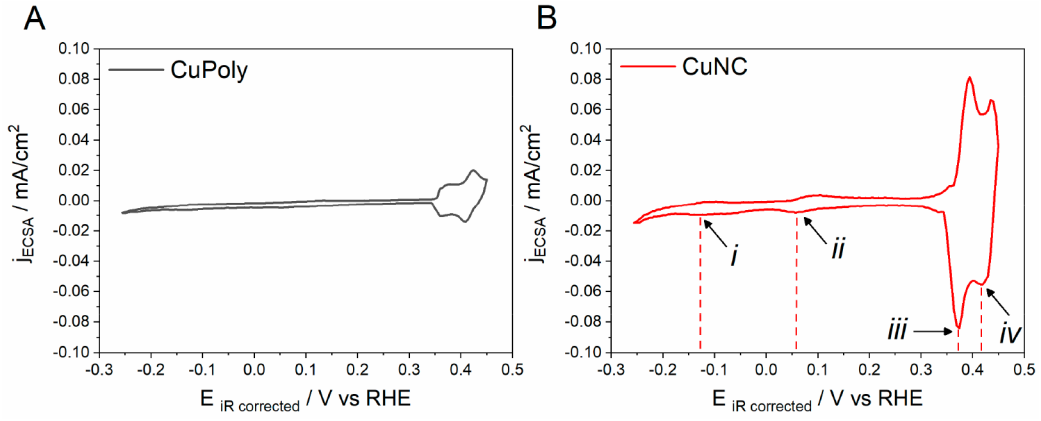

Figure 2. Cyclic voltammograms of Cu polycrystalline (CuPoly; A) and Cu nanocube (CuNC; B) electrodes in 0.1 M NaOH, under an Ar atmosphere, at a scan rate of 50 mV s^{-1}.

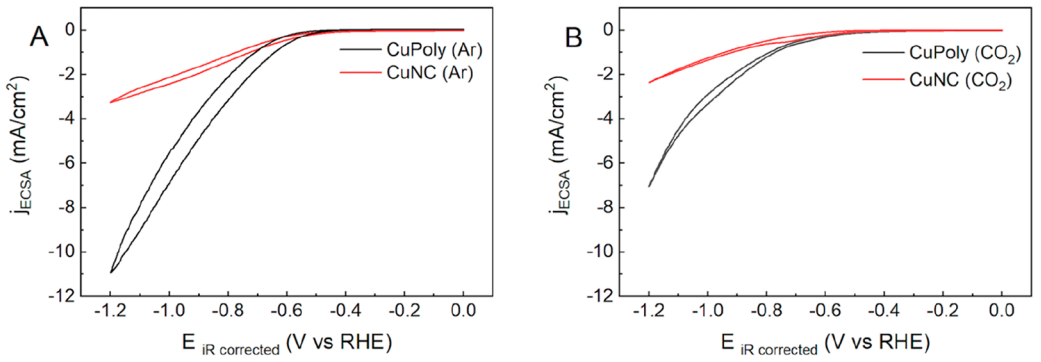

Figure 3. Cyclic voltammograms of CuPoly and CuNC under Ar (A) and CO_2 (B) atmospheres in 0.1 M $KHCO_{3(aq)}$ at a scan rate of 50 mV s^{-1}.

nanocubes of ∼70 nm (CuNC, Figure 1C) and nanodendrites of ∼300 nm (CuND, Figure 1D) were obtained, respectively. These materials are referred to as oxide-derived Cu electrodes (Cu_xO), as they are metallic electrodes resulting from the reduction of an oxide.[43] They are composed of mostly metallic copper (Cu^0) and copper oxide (Cu(I)), with a higher proportion of the latter being present than in CuPoly.[40,44]

The synthesized Cu_xO-derived electrode surfaces were also characterized electrochemically by performing cyclic voltammetry (CV) in a blank electrolyte (0.1 M NaOH) between −0.25 and 0.45 V versus RHE. The obtained profiles for CuPoly and CuNC are shown in Figure 2, whereas CuNS and CuND profiles are depicted in Figure S2.

For all Cu surfaces, multiple well-defined peaks are observed in the potential range between −0.25 V < E < 0.45 V versus RHE, and the double layer for all electrodes are similar, in agreement with the literature for metallic copper.[45] A peak at −0.13 V (Figure 2B,*i*) is observed on the CuNC (Figure 2B) and CuND (Figure S2) electrodes, and it corresponds to the adsorption/desorption of OH^- species on (100) terraces, providing evidence for the increased exposure of this facet.[17,46] The peak at 0.06 V (Figure 2B,*ii*) corresponds to the adsorption/desorption of OH^- on the (111) terraces.

The presence of defects or low coordinate sites are evidenced by the small voltammetric feature at 0.30 V versus RHE,[47,48] appearing before the prominent features centered at 0.37 V (Figure 2B, *iii*) and 0.42 V (Figure 2B, *iv*), which are due to the redox activity of Cu to Cu_2O over different domains of the copper surface.[45] For Cu(100) crystallographic orientation, the same peaks are attributed to the oxidation of (100) domains,[48] which agrees with the fact that CuNC (Figure 2B) has more well-defined peaks in this potential region.

As Cu electrodes with (100) crystallographic orientation are well-known to possess a high selectivity toward the C−C coupling reaction for the CO_2RR,[44,45,47,49,50] all subsequent results are related only to CuNC in comparison to CuPoly.

3.2. Electrochemical CO_2 Reduction. *3.2.1. Effect of the Solvent.* To better understand how electrode structure and electrolyte composition affect both product distribution and the competition between CO_2RR and HER on the Cu electrode, we studied these reactions in aqueous (0.1 M $KHCO_{3(aq)}$, ∼55 M of H_2O) and organic (0.1 M TEACl in CH_3CN) electrolytes through cyclic voltammetry (CV) using CuPoly and CuNC electrodes.

Figure 3 compares the CVs for CuPoly(black line) and CuNC (red line) in an aqueous solution. Hydrogen evolution was observed in an argon-purged electrolyte, as shown in Figure 3A, where an increase in cathodic current density due to water reduction is observed at around −0.55 V versus RHE, for both electrodes.

We also performed cyclic voltammetry in a CO_2 atmosphere (Figure 3B) in order to distinguish the currents from HER and CO_2RR. In aqueous solution, a slightly lower reduction current density is observed on both CuPoly and CuNC electrodes, compared to the Ar-saturated electrolyte, suggesting the strong competition between the CO_2RR and HER.

In both Ar and CO_2 electrochemical conditions, the CuPoly electrode showed a 4-fold higher current density than CuNC. This difference is at least partially associated with a lower

https://doi.org/10.1021/acs.jpcc.3c03257
J. Phys. Chem. C 2023, 127, 14518−14527

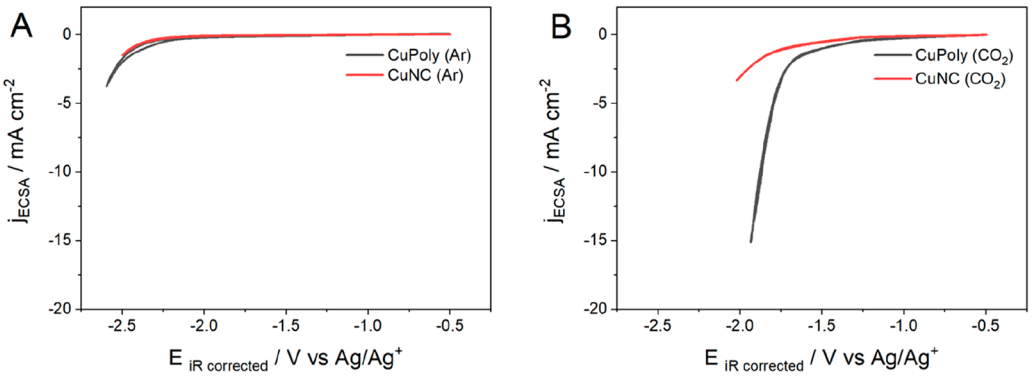

Figure 4. Cyclic voltammograms of CuPoly and CuNC electrodes in MeCN (0.1 M TEACl) under Ar (A) and CO_2 (B) atmospheres at a scan rate of 50 mV s^{-1}.

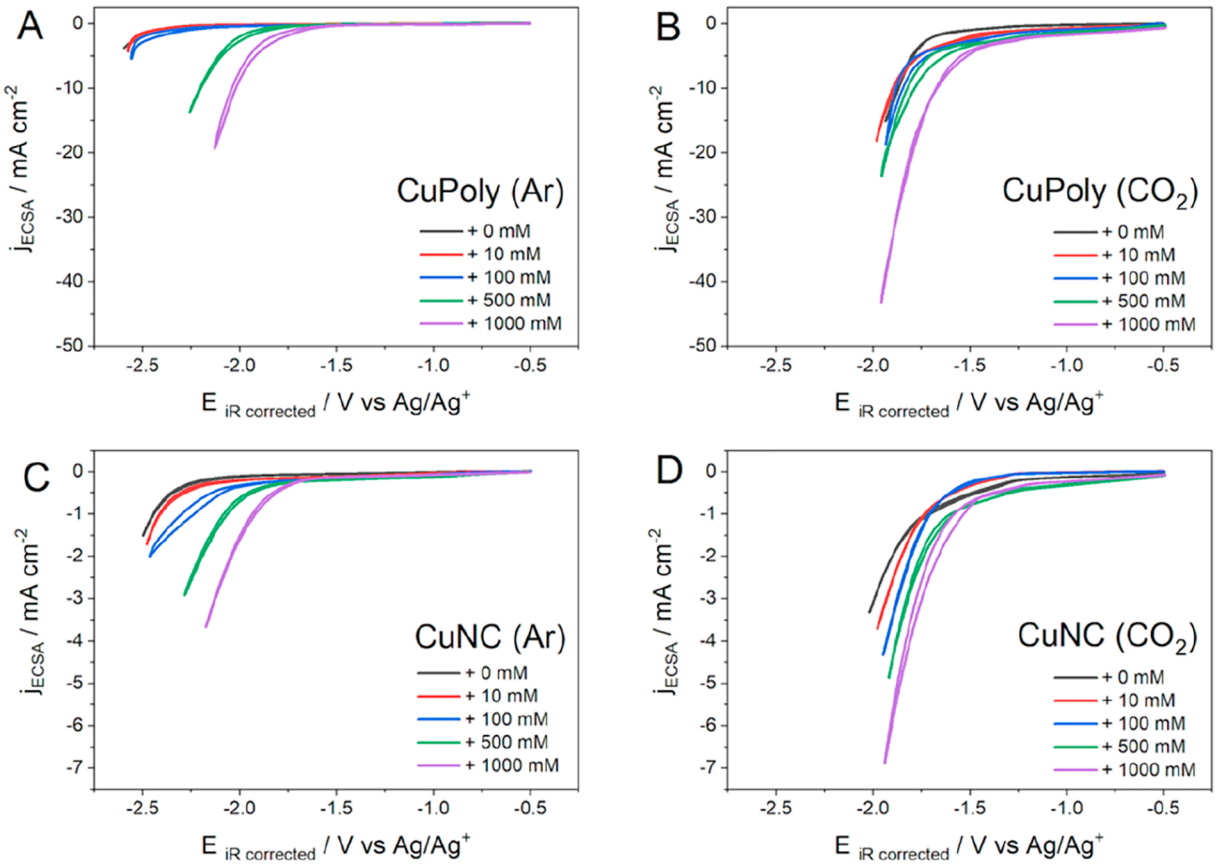

Figure 5. Cyclic voltammograms for CuPoly and CuNC under Ar (A, C) and CO_2 (B, D), respectively, in acetonitrile (0.1 M TEACl). Scan rate: 50 mV s^{-1}.

partial current density for HER for CuNC electrode.[29] Our findings agree with previous work in which Cu(110), which is closer to the copper polycrystalline surface, was shown to be more active for hydrogen evolution than Cu(100).[51]

As mentioned, we also studied the CO_2RR in acetonitrile solvent to minimize its competition with HER. Figure 4A compares the CVs of both CuPoly and CuNC electrodes in an argon-purged acetonitrile solvent. On both electrodes, an increase in current density is observed only at potentials more negative than −2.0 V versus Ag/Ag^+. Such increase in current is most likely due to the reduction of residual water present in the acetonitrile electrolyte solution.

Unlike in an aqueous electrolyte, where the competition between the CO_2RR and HER on Cu often leads to a lower overall current compared to a CO_2-free electrolyte, in acetonitrile, the CO_2RR (Figure 4B) leads to higher reduction currents than in Ar-saturated electrolyte (Figure 4A), suggesting the absence of strong competition between both reactions due to low HER activity and to a higher solubility of CO_2 in acetonitrile compared to water.

The slightly higher current densities observed in Figure 4B in comparison with aqueous electrolytes (Figure 3B), especially on CuPoly (black line), suggest that, in acetonitrile solvent, CO appears to desorb more easily from the electrode surface. Such an observation will be reinforced with the online

https://doi.org/10.1021/acs.jpcc.3c03257
J. Phys. Chem. C 2023, 127, 14518−14527

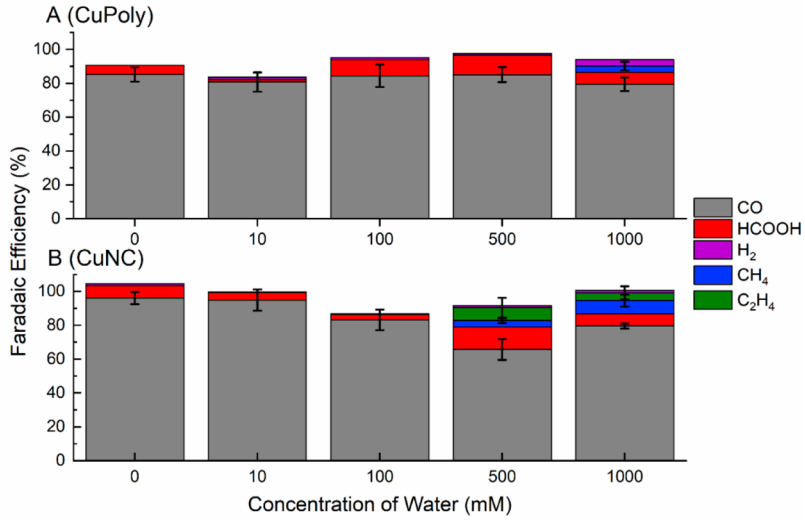

Figure 6. Faradaic efficiencies of CuPoly(A) and CuNC (B) at varying concentrations of water, determined by online gas chromatography at −2.0 V vs Ag/Ag^+ for 90 min.

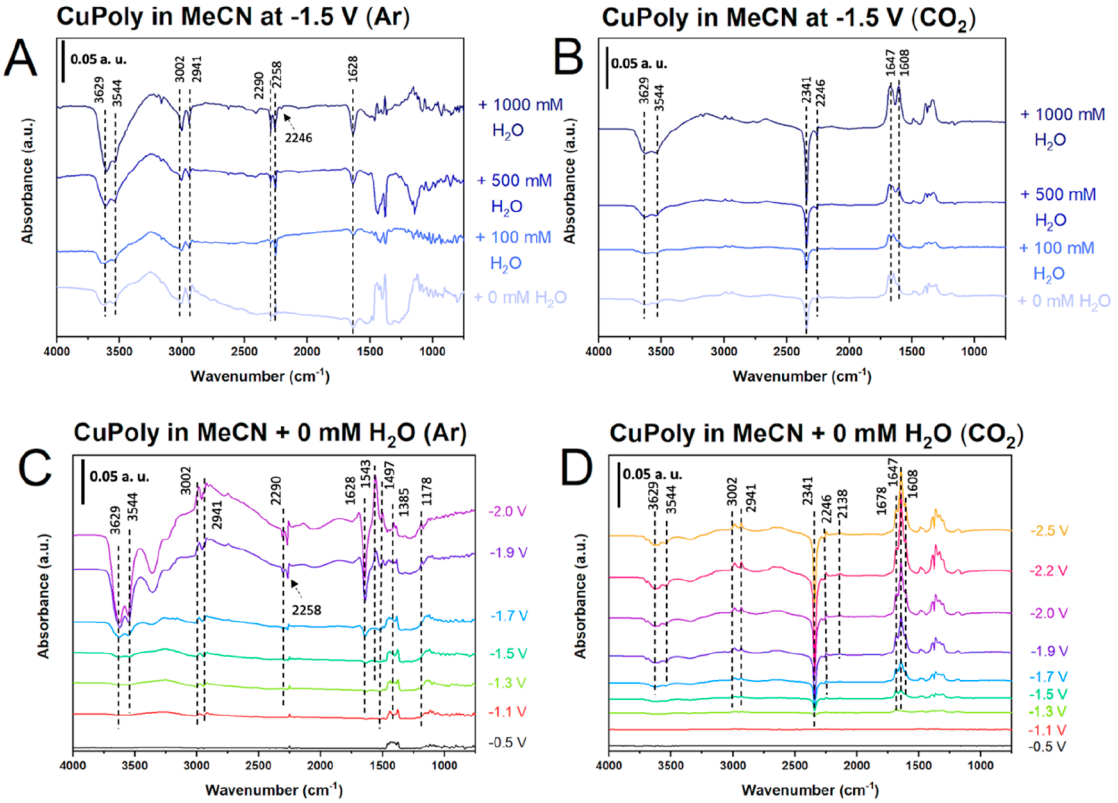

Figure 7. FTIR spectra for hydrogen evolution (A, C) and CO_2 reduction (B, D) at CuPoly electrode in 0.1 M TEACl in CH_3CN at the indicated water content and applied potentials. Reference spectrum was taken at −0.1 V vs Ag/Ag^+.

gas chromatography analysis and in situ FTIR spectroscopy results, to be further discussed below. As in aqueous electrolyte, CuPoly shows a higher CO_2RR activity than CuNC, although it is not clear if this is for the same reason.

3.2.2. Effect of the Water Content on Activity and Selectivity. We further studied the role of water during HER and CO_2RR in acetonitrile by varying its concentration in the electrolyte. Figure 5 shows the cyclic voltammograms obtained for HER and the CO_2RR on CuPoly and CuNC in acetonitrile with different water concentrations. The results show that independent of the Cu surface, the HER (Figure 5A,C) is more sensitive to the water content than the CO_2RR (Figure 5B,D). Moreover, the results in Figure 5 suggest that water is not directly involved in the rate-determining step of CO_2 reduction.

To probe the effect of water on the product distribution during the CO_2RR in acetonitrile solvent, chronoamperometry combined with online GC was carried out with different water concentrations on both CuPoly and CuNC electrodes. Product distributions and the corresponding Faradaic Efficiencies (FE)

https://doi.org/10.1021/acs.jpcc.3c03257
J. Phys. Chem. C 2023, 127, 14518−14527

are depicted in Figure 6, whereas the partial currents for the related products are presented in Figure S3, which confirms higher currents for CuNC than for CuPoly.

The results in Figure 6 show that on both CuPoly and CuNC electrodes, CO is the major product from the CO_2 reduction in acetonitrile, regardless of the water concentration. This observation is in line with the small effect of the water concentration on the activity of CO_2RR (Figure 5B,D). Similar to the findings in aqueous media for Cu(100) and Cu-oxide derived in aqueous media,[25,29,43,52−54] CuNC was the only surface capable of promoting C−C coupling during CO_2RR in acetonitrile toward ethylene (C_2H_4), but only if enough water has been added (>500 mM) to the electrolyte. FE often does not reach 100%, which is thought to be due to a small contribution of carbonate formation.

Interestingly, the online GC analysis shows that the presence of CO_2 suppresses hydrogen evolution because little to no H_2 is detected, even at higher amounts of water, where the HER current in the absence of CO_2 is in fact quite substantial (see the "+1000 mM" curves in Figure 5A,C). Only on CuPoly with 1000 mM H_2O, there is a measurable FE for hydrogen, but it is still not higher than a few percent. Like in aqueous electrolytes, CuPoly is more active for HER than CuNC.

By comparison, experiments in bicarbonate solution using very similar copper polycrystalline and Cu nanocube electrodes showed a FE for H_2 of around 75% and 50%, respectively, during CO_2 reduction.[43]

3.2.3. In Situ FTIR Analysis. To better understand the effect of the water content on the competition between hydrogen evolution and CO_2 reduction, the reactions in acetonitrile were also investigated by in situ FTIR spectroscopic studies on the CuPoly electrode.

The in situ FTIR spectra on CuPoly under an Ar atmosphere as a function of water content and applied potential are given in Figure 7A and C, respectively. Negative bands at 3629−3544 and 1628 cm^{-1}, which are assigned to OH stretching and bending modes of residual water present in the acetonitrile solvent,[55] respectively, become evident at potentials more negative than −1.5 V versus Ag/Ag^+ (Figure 7C), in agreement with the cyclic voltammograms shown in Figure 4A. Their intensity also increases with increasing water concentration (Figure 7A), suggesting water is being reduced to produce hydrogen via $2H_2O + 2e^- \rightarrow H_2 + 2OH^-$ reaction.

The spectra show common bands at around 3002−2941 cm^{-1}, which are assigned to CH stretching from TEA^+ and acetonitrile, respectively.[56] In the C−N region of the spectra we observe three bands at 2290, 2258, and 2246 cm^{-1},[57] which are less evident in the CO_2 atmosphere. The bands at 2290 and 2246 cm^{-1} are assigned to the C−N stretching from acetonitrile free from interactions with anions,[21] whereas the band at 2258 cm^{-1} is attributed to C−N groups from acetonitrile that interacts with chloride anion, similarly to what has been observed for BF_4^- and ClO_4^- groups at Cu and Pt electrodes, respectively.[21,58]

The positive bands in the region of 1543, 1497/1385, and 1178 cm^{-1} are assigned to C═O stretching, NH_2 stretching, and NH_2 bending modes, respectively, suggesting acetonitrile is decomposing to acetamide.[21] These results agree with previous reports that found that, at more negative potentials, acetonitrile is decomposed into acetamide via a nucleophile attack of OH^- species generated during reduction of residual water[21,59] We observed the related bands at slightly less negative potentials because before applying potentials for either HER or CO_2RR, we performed a single voltametric scan in order to check the electrode surface in the spectro-electrochemical cell; however, this does not affect the interpretation of our data.

Additional bands are obtained when the electrolyte is saturated with CO_2, as shown in Figure 7B,D. At −1.3 V (Figure 7D), the spectra show a negative band at 2341 cm^{-1} corresponding to CO_2 consumption.[21] This band becomes more intense with increasing amounts of water (Figure 7B) and at potentials more negative than −1.5 V (Figure 7D), which corresponds to the onset potential for CO_2 reduction suggested by cyclic voltammetry (Figure 4B).

A high number of positive bands related to the formation of carbonyl species are observed in the wavenumber region around 1678−1608 cm^{-1} (Figure 7D).[21] These bands increase as a function of potential at the same time as the negative band related to CO_2 consumption increases, indicating those bands correspond to products from the CO_2RR. More water in the system increases the production of the OH^- species due to water reduction, which in the presence of CO_2 leads to the formation of carbonate and bicarbonate (HCO_3^-) species, as observed by the increase of the bands at 1608 cm^{-1}, in agreement with previous literature.[21] Once carbonate was not quantified as a final product, it justifies why the FE often does not reach 100% (Figure 6).

An interesting feature is revealed concerning the competition between the HER and the CO_2RR in acetonitrile solvent. We found that the presence of CO_2 in the acetonitrile electrolyte completely suppresses the band at 1628 cm^{-1}, assigned to OH bending of water, while the bands at 3629−3544 cm^{-1} (OH stretching) are less intense than observed in the absence of CO_2 (Figure 7A,C). These results confirm that in acetonitrile solvent, the presence of CO_2 inhibits H_2O accumulation at the surface and therefore its reduction to H_2. We observe a small band at 2138 cm^{-1} (Figure 7D) that is assigned to the C−O stretching mode of CO gas, in agreement with the online gas chromatography analysis (Figure 6). In fact, in aprotic solvents, CO is formed as a product from CO_2RR; however, due to its low solubility in acetonitrile, FTIR has a limited sensitivity for identifying CO.[21] Unlike in aqueous solvent, where bridged and linearly adsorbed CO on Cu electrode were observed at 1800−1900 and 2050−2080 cm^{-1}, respectively,[60] our results do not show any band in this region of the spectra, confirming the CO-coverage on Cu electrode in acetonitrile is very low, making it difficult to be identified.

4. DISCUSSION AND CONCLUSION

Through a combination of cyclic voltammetry with online GC and in situ FTIR experiments, our results reveal that, similar to aqueous media,[27,37] CO_2RR selectivity toward C_{2+} products in acetonitrile is dependent on the structure and electrolyte composition. We found that CuNC is the only surface capable of producing 10% FE of ethylene if there is enough water present in the electrolyte (>500 mM). It appears that, in general, the qualitative effect of surface structure is the same in water and acetonitrile. Previous work done by Scholten et al.[29] showed that flat electrodes favor HER over CO_2RR and that only with the introduction of defects, as is the case of CuNC, the selectivity shifts toward C_{2+} hydrocarbons. Our results are also in accordance with previous work, which has shown that Cu(110) surfaces, which are more similar to copper polycrystalline surface, are more active for hydrogen

https://doi.org/10.1021/acs.jpcc.3c03257
J. Phys. Chem. C 2023, 127, 14518−14527

evolution.[51] This explains why CuPoly is more active for hydrogen evolution than CuNC in both electrolytes. Interestingly, whereas in aqueous media, CO_2RR suppresses hydrogen evolution on both CuPoly and CuNC electrodes, the opposite is true in acetonitrile. In contrast to aqueous electrolytes, in acetonitrile solvent, the currents obtained for CuPoly and CuNC in a CO_2-saturated electrolyte are higher than the currents obtained in an argon-purged electrolyte. Another remarkable difference is the quantitative selectivity toward CO, which is >85% on both CuPoly and CuNC in acetonitrile, whereas it is much lower in aqueous media on both CuPoly and CuNC (~9.4% and 13.6%, respectively).

These results suggest that, in acetonitrile, CO desorbs much easier from the electrode surface than in aqueous media. The exact reason for this is not clear, but may be related to the stronger interaction of acetonitrile with the Cu, which then drives the CO off the surface. Remarkably, the addition of water to acetonitrile has little quantitative and almost no qualitative effect on the activity and selectivity of CO_2RR. This strongly suggest that water is not strongly involved in rate-determining step of CO_2RR in acetonitrile. Only at the highest water concentrations and at the CuNC surface, the CO coverage becomes high enough that a small amount of C_{2+} products are formed.

■ ASSOCIATED CONTENT

Supporting Information

The Supporting Information is available free of charge at https://pubs.acs.org/doi/10.1021/acs.jpcc.3c03257.

CVs of Fc/Fc^+ in 0.1 M TEACl with 0 or 1 M of H_2O, saturated with Ar or CO_2; CVs of Cu nanospheres (CuNS) and Cu nanodendrites (CuND) electrodes in 0.1 M NaOH; Partial currents corresponding to various products recorded for the conditions reported in Figure 6; CVs of Cu nanocubes (CuNC) before and after electrolysis in 0.1 M NaOH (PDF)

■ AUTHOR INFORMATION

Corresponding Author

Amanda C. Garcia − *Van't Hoff Institute for Molecular Sciences, University of Amsterdam, 1098 XH Amsterdam, The Netherlands;* orcid.org/0000-0002-0242-9244; Email: a.c.garcia@uva.nl

Authors

Connor Deacon-Price − *Van't Hoff Institute for Molecular Sciences, University of Amsterdam, 1098 XH Amsterdam, The Netherlands*

Alisson H. M. da Silva − *Leiden Institute of Chemistry, Leiden University, 2300 RA Leiden, The Netherlands*

Cássia S. Santana − *Van't Hoff Institute for Molecular Sciences, University of Amsterdam, 1098 XH Amsterdam, The Netherlands*

Marc T. M. Koper − *Leiden Institute of Chemistry, Leiden University, 2300 RA Leiden, The Netherlands;* orcid.org/0000-0001-6777-4594

Complete contact information is available at: https://pubs.acs.org/10.1021/acs.jpcc.3c03257

Notes

The authors declare no competing financial interest.

■ ACKNOWLEDGMENTS

The research of C.D.P. and A.C.G. was carried out under Project Number ECCM.TT.ECCM.008 and the research of C.S.S. and A.C.G. was developed under Project Number KICH1.ED04.20.026. Both research projects were carried out in the framework of the Electrochemical Conversion and Materials (ECCM) program and received funding from the Dutch Research Council (NWO). The research of A.H.M.d.S. and M.T.M.K. was carried out under Project Number ENPPS.IPP.019.002 in the framework of the Research Program of the Materials innovation institute (M2i; www.m2i.nl) and received funding from Tata Steel Nederland Technology BV and the Dutch Research Council (NWO) in the framework of the ENW PPP Fund for the Top Sectors and from the Ministry of Economic Affairs in the framework of the "PPS-Toeslagregeling".

■ REFERENCES

(1) Hori, Y.; Kikuchi, K.; Suzuki, S. Production of CO and CH_4 in Electrochemical Reduction of CO_2 at Metal Electrodes in Aqueous Hydrogencarbonate Solution. *Chem. Lett.* **1985**, *14* (11), 1695−1698.

(2) Birdja, Y. Y.; Pérez-Gallent, E.; Figueiredo, M. C.; Göttle, A. J.; Calle-Vallejo, F.; Koper, M. T. M. Advances and Challenges in Understanding the Electrocatalytic Conversion of Carbon Dioxide to Fuels. *Nat. Energy* **2019**, *4* (9), 732−745.

(3) Nam, D.-H.; de Luna, P.; Rosas-Hernández, A.; Thevenon, A.; Li, F.; Agapie, T.; Peters, J. C.; Shekhah, O.; Eddaoudi, M.; Sargent, E. H. Molecular Enhancement of Heterogeneous CO_2 Reduction. *Nat. Mater.* **2020**, *19* (3), 266−276.

(4) Monteiro, M. C. O.; Dattila, F.; López, N.; Koper, M. T. M. The Role of Cation Acidity on the Competition between Hydrogen Evolution and CO_2 Reduction on Gold Electrodes. *J. Am. Chem. Soc.* **2022**, *144* (4), 1589−1602.

(5) Zheng, T.; Jiang, K.; Wang, H. Recent Advances in Electrochemical CO_2-to-CO Conversion on Heterogeneous Catalysts. *Adv. Mater.* **2018**, *30* (48), 1802066.

(6) Hori, Y.; Murata, A.; Takahashi, R. Formation of Hydrocarbons in the Electrochemical Reduction of Carbon Dioxide at a Copper Electrode in Aqueous Solution. *J. Chem. Soc., Faraday Trans. 1* **1989**, *85* (8), 2309−2326.

(7) Yang, H.; Kaczur, J. J.; Sajjad, S. D.; Masel, R. I. Performance and Long-Term Stability of CO_2 Conversion to Formic Acid Using a Three-Compartment Electrolyzer Design. *J. CO_2 Util.* **2020**, *42*, 101349.

(8) Nitopi, S.; Bertheussen, E.; Scott, S. S.; Liu, X.; Engstfeld, A. K.; Horch, S.; Seger, B.; Stephens, I. E. L.; Chan, K.; Norskov, J. K.; et al. Progress and Perspectives of electrochemical CO_2 reduction on copper in aqueous electrolyte. *Chem. Rev.* **2019**, *119* (12), 7610−7672.

(9) Zhang, Y.-J.; Sethuraman, V.; Michalsky, R.; Peterson, A. Competiiton between CO_2 reduction and H_2 evolution on transition-metal electrocatalysts. *ACS Catal.* **2014**, *4* (10), 3742−3748.

(10) Hori, Y. Electrochemical CO_2 Reduction on Metal Electrodes. In *Modern Aspects of Electrochemistry*; Vayenas, C. G., White, R. E., Gamboa-Aldeco, M. E., Eds.; Springer: New York, NY, 2008; pp 89−189.

(11) Tan, W.; Cao, B.; Xiao, W.; Zhang, M.; Wang, S.; Xie, S.; Xie, D.; Cheng, F.; Guo, Q.; Liu, P. Electrochemical Reduction of CO_2 on Hollow Cubic Cu_2O@Au Nanocomposites. *Nanoscale Res. Lett.* **2019**, *14* (1), 63.

(12) Goyal, A.; Koper, M. T. M. The Interrelated Effect of Cations and Electrolyte pH on the Hydrogen Evolution Reaction on Gold Electrodes in Alkaline Media. *Angew. Chem., Int. Ed.* **2021**, *60* (24), 13452−13462.

(13) Waegele, M. M.; Gunathunge, C. M.; Li, J.; Li, X. How cations affect the electric double layer and the rates and selectivity of electrocatalytic processes. *J. Chem. Phys.* **2019**, *151*, 160902.

(14) Marcandalli, G.; Goyal, A.; Koper, M. T. M. Electrolyte Effects on the Faradaic Efficiency of CO_2 Reduction to CO on a Gold Electrode. *ACS Catal.* **2021**, *11* (9), 4936−4945.
(15) Marcandalli, G.; Monteiro, M. C. O.; Goyal, A.; Koper, M. T. M. Electrolyte Effects on CO_2 Electrochemical Reduction to CO. *Acc. Chem. Res.* **2022**, *55* (14), 1900−1911.
(16) Monteiro, M. C. O.; Dattila, F.; Hagedoorn, B.; García-Muelas, R.; López, N.; Koper, M. T. M. Absence of CO_2 Electroreduction on Copper, Gold and Silver Electrodes without Metal Cations in Solution. *Nat. Catal. 2021 4:8* **2021**, *4* (8), 654−662.
(17) Raaijman, S. J.; Arulmozhi, N.; Koper, M. T. M. Morphological Stability of Copper Surfaces under Reducing Conditions. *ACS Appl. Mater. Interfaces* **2021**, *13* (41), 48730−48744.
(18) Callahan, T.; Masi, D.; Xiao, D. Designing Catalytic Sites on Surfaces with Optimal H-Atom Binding via Atom Doping Using the Inverse Molecular Design Approach. *J. Phys. Chem. B* **2019**, *123* (48), 10252−10259.
(19) Madhavan, P. v; Whitten, J. L. Hydrogen Adsorption on Copper: Embedding Theory Based on Orbital Localization. *Surf. Sci.* **1981**, *112* (1), 38−51.
(20) Tabatabaei, J.; Sakakini, B. H.; Watson, M. J.; Waugh, K. C. The Detailed Kinetics of the Adsorption of Hydrogen on Polycrystalline Copper Studied by Reactive Frontal Chromatography. *Catal. Lett.* **1999**, *59* (2), 151−155.
(21) Figueiredo, M. C.; Ledezma-Yanez, I.; Koper, M. T. M. In Situ Spectroscopic Study of CO_2 Electroreduction at Copper Electrodes in Acetonitrile. *ACS Catal.* **2016**, *6* (4), 2382−2392.
(22) Amatore, C.; Savéant, J. M. Mechanism and Kinetic Characteristics of the Electrochemical Reduction of Carbon Dioxide in Media of Low Proton Availability. *J. Am. Chem. Soc.* **1981**, *103* (17), 5021−5023.
(23) Uemoto, N.; Furukawa, M.; Tateishi, I.; Katsumata, H.; Kaneco, S. Electrochemical Carbon Dioxide Reduction in Methanol at Cu and Cu_2O-Deposited Carbon Black Electrodes. *ChemEngineering 2019, Vol. 3, Page 15* **2019**, *3* (1), 15.
(24) Schouten, K. J. P.; Qin, Z.; Pérez Gallent, E.; Koper, M. T. M. Two Pathways for the Formation of Ethylene in CO Reduction on Single-Crystal Copper Electrodes. *J. Am. Chem. Soc.* **2012**, *134* (24), 9864−9867.
(25) Hahn, C.; Hatsukade, T.; Kim, Y.-G.; Vailionis, A.; Baricuatro, J. H.; Higgins, D. C.; Nitopi, S. A.; Soriaga, M. P.; Jaramillo, T. F. Engineering Cu surfaces for the electrocatalytic conversion of CO_2: Controlling selectivity toward oxygenates and hydrocarbons. *Proc. Natl. Acad. Sci. U.S.A.* **2017**, *114* (23), 5918−5923.
(26) Pérez-Gallent, E.; Figueiredo, M. C.; Calle-Vallejo, F.; Koper, M. T. M. Spectroscopic Observation of a Hydrogenated CO Dimer Intermediate During CO Reduction on Cu(100) Electrodes. *Angew. Chem., Int. Ed.* **2017**, *56* (13), 3621−3624.
(27) Schouten, K. J. P.; Kwon, Y.; van der Ham, C. J. M.; Qin, Z.; Koper, M. T. M. A New Mechanism for the Selectivity to C_1 and C_2 Species in the Electrochemical Reduction of Carbon Dioxide on Copper Electrodes. *Chem. Sci.* **2011**, *2* (10), 1902−1909.
(28) Hori, Y.; Takahashi, I.; Koga, O.; Hoshi, N. Electrochemical Reduction of Carbon Dioxide at Various Series of Copper Single Crystal Electrodes. *J. Mol. Catal. A: Chem.* **2003**, *199* (1), 39−47.
(29) Scholten, F.; Nguyen, K. L. C.; Bruce, J. P.; Heyde, M.; Roldan Cuenya, B. Identifying Structure−Selectivity Correlations in the Electrochemical Reduction of CO_2: A Comparison of Well-Ordered Atomically Clean and Chemically Etched Copper Single-Crystal Surfaces. *Angew. Chem., Int. Ed.* **2021**, *60* (35), 19169−19175.
(30) Li, C. W.; Kanan, M. W. CO_2 Reduction at Low Overpotential on Cu Electrodes Resulting from the Reduction of Thick Cu_2O Films. *J. Am. Chem. Soc.* **2012**, *134* (17), 7231−7234.
(31) Bagger, A.; Ju, W.; Varela, A. S.; Strasser, P.; Rossmeisl, J. Electrochemical CO_2 Reduction: A Classification Problem. *ChemPhysChem* **2017**, *18* (22), 3266−3273.
(32) Huang, Y.; Handoko, A. D.; Hirunsit, P.; Yeo, B. S. Electrochemical Reduction of CO_2 Using Copper Single-Crystal Surfaces: Effects of CO* Coverage on the Selective Formation of Ethylene. *ACS Catal.* **2017**, *7* (3), 1749−1756.
(33) Hanselman, S.; Koper, M. T. M.; Calle-Vallejo, F. Computational Comparison of Late Transition Metal (100) Surfaces for the Electrocatalytic Reduction of CO to C_2 Species. *ACS Energy Lett.* **2018**, *3* (5), 1062−1067.
(34) Gattrell, M.; Gupta, N.; Co, A. A Review of the Aqueous Electrochemical Reduction of CO_2 to Hydrocarbons at Copper. *J. Electroanal. Chem.* **2006**, *594* (1), 1−19.
(35) Calle-Vallejo, F.; Koper, M. T. M. Theoretical Considerations on the Electroreduction of CO to C_2 Species on Cu(100) Electrodes. *Angew. Chem., Int. Ed.* **2013**, *52* (28), 7282−7285.
(36) Montoya, J. H.; Shi, C.; Chan, K.; Nørskov, J. K. Theoretical Insights into a CO Dimerization Mechanism in CO_2 Electroreduction. *J. Phys. Chem. Lett.* **2015**, *6* (11), 2032−2037.
(37) Schouten, K. J. P.; Pérez Gallent, E.; Koper, M. T. M. The Influence of pH on the Reduction of CO and CO_2 to Hydrocarbons on Copper Electrodes. *J. Electroanal. Chem.* **2014**, *716*, 53−57.
(38) Kortlever, R.; Peters, I.; Balemans, C.; Kas, R.; Kwon, Y.; Mul, G.; Koper, M. T. M. Palladium−Gold Catalyst for the Electrochemical Reduction of CO_2 to C_1−C_5 Hydrocarbons. *ChemComm* **2016**, *52* (67), 10229−10232.
(39) García, G.; Rodríguez, P.; Rosca, V.; Koper, M. T. M. Fourier Transform Infrared Spectroscopy Study of CO Electro-Oxidation on Pt(111) in Alkaline Media. *Langmuir* **2009**, *25* (23), 13661−13666.
(40) Roberts, F. S.; Kuhl, K. P.; Nilsson, A. High Selectivity for Ethylene from Carbon Dioxide Reduction over Copper Nanocube Electrocatalysts. *Angew. Chem.* **2015**, *127* (17), 5268−5271.
(41) Li, C. W.; Ciston, J.; Kanan, M. W. Electroreduction of Carbon Monoxide to Liquid Fuel on Oxide-Derived Nanocrystalline Copper. *Nature* **2014**, *508* (7497), 504−507.
(42) Verdaguer-Casadevall, A.; Li, C. W.; Johansson, T. P.; Scott, S. B.; McKeown, J. T.; Kumar, M.; Stephens, I. E. L.; Kanan, M. W.; Chorkendorff, I. Probing the Active Surface Sites for CO Reduction on Oxide-Derived Copper Electrocatalysts. *J. Am. Chem. Soc.* **2015**, *137* (31), 9808−9811.
(43) da Silva, A. H. M.; Raaijman, S. J.; Santana, C. S.; Assaf, J. M.; Gomes, J. F.; Koper, M. T. M. Electrocatalytic CO_2 Reduction to C_{2+} Products on Cu and CuxZny Electrodes: Effects of Chemical Composition and Surface Morphology. *J. Electroanal. Chem.* **2021**, *880*, 114750.
(44) Arán-Ais, R. M.; Rizo, R.; Grosse, P.; Algara-Siller, G.; Dembélé, K.; Plodinec, M.; Lunkenbein, T.; Chee, S. W.; Cuenya, B. R. Imaging Electrochemically Synthesized Cu_2O Cubes and Their Morphological Evolution under Conditions Relevant to CO_2 Electroreduction. *Nat. Commun.* **2020**, *11* (1), 3489.
(45) P. Schouten, K. J.; Gallent, E. P.; Koper, M. T. M. The Electrochemical Characterization of Copper Single-Crystal Electrodes in Alkaline Media. *J. Electroanal. Chem.* **2013**, *699*, 6−9.
(46) Raaijman, S. J.; Arulmozhi, N.; da Silva, A. H. M.; Koper, M. T. M. Clean and Reproducible Voltammetry of Copper Single Crystals with Prominent Facet-Specific Features Using Induction Annealing. *J. Electrochem. Soc.* **2021**, *168* (9), 096510.
(47) Arán-Ais, R. M.; Scholten, F.; Kunze, S.; Rizo, R.; Roldan Cuenya, B. The Role of in Situ Generated Morphological Motifs and Cu(I) Species in C_{2+} Product Selectivity during CO_2 Pulsed Electroreduction. *Nat. Energy* **2020**, *5* (4), 317−325.
(48) Engstfeld, A. K.; Maagaard, T.; Horch, S.; Chorkendorff, I.; Stephens, I. E. L. Polycrystalline and Single-Crystal Cu Electrodes: Influence of Experimental Conditions on the Electrochemical Properties in Alkaline Media. *Chem.—Eur. J.* **2018**, *24* (67), 17743−17755.
(49) Todorova, T. K.; Schreiber, M. W.; Fontecave, M. Mechanistic Understanding of CO_2 Reduction Reaction (CO2RR) Toward Multicarbon Products by Heterogeneous Copper-Based Catalysts. *ACS Catal.* **2020**, *10* (3), 1754−1768.
(50) Kim, D.; Lee, S.; Ocon, J. D.; Jeong, B.; Lee, J. K.; Lee, J. Insights into an Autonomously Formed Oxygen-Evacuated Cu_2O

Electrode for the Selective Production of C_2H_4 from CO_2. *Phys. Chem. Chem. Phys.* **2015**, *17* (2), 824−830.
(51) Tiwari, A.; Heenen, H. H.; Bjørnlund, A. S.; Maagaard, T.; Cho, E.; Chorkendorff, I.; Kristoffersen, H. H.; Chan, K.; Horch, S. Fingerprint Voltammograms of Copper Single Crystals under Alkaline Conditions: A Fundamental Mechanistic Analysis. *J. Phys. Chem. Lett.* **2020**, *11* (4), 1450−1455.
(52) Zhan, C.; Dattila, F.; Rettenmaier, C.; Bergmann, A.; Kühl, S.; García-Muelas, R.; López, N.; Cuenya, B. R. Revealing the CO Coverage-Driven C-C Coupling Mechanism for Electrochemical CO_2 Reduction on Cu_2O Nanocubes via Operando Raman Spectroscopy. *ACS Catal.* **2021**, *11* (13), 7694−7701.
(53) Arán-Ais, R. M.; Gao, D.; Roldan Cuenya, B. Structure- and Electrolyte-Sensitivity in CO_2 Electroreduction. *Acc. Chem. Res.* **2018**, *51* (11), 2906−2917.
(54) Kortlever, R.; Shen, J.; Schouten, K. J. P.; Calle-Vallejo, F.; Koper, M. T. M. Catalysts and Reaction Pathways for the Electrochemical Reduction of Carbon Dioxide. *J. Phys. Chem. Lett.* **2015**, *6* (20), 4073−4082.
(55) Kitadai, N.; Sawai, T.; Tonoue, R.; Nakashima, S.; Katsura, M.; Fukushi, K. Effects of Ions on the OH Stretching Band of Water as Revealed by ATR-IR Spectroscopy. *J. Solution Chem.* **2014**, *43* (6), 1055−1077.
(56) Irish, D. E.; Hill, I. R.; Archambault, P.; Atkinson, G. F. Investigations of Electrode Surfaces in Acetonitrile Solutions Using Surface-Enhanced Raman Spectroscopy. *J. Solution Chem.* **1985**, *14* (3), 221−243.
(57) Marinković, N. S.; Hecht, M.; Loring, J. S.; Fawcett, W. R. A SNIFTIRS Study of the Diffuse Double Layer at Single Crystal Platinum Electrodes in Acetonitrile. *Electrochim. Acta* **1996**, *41* (5), 641−651.
(58) Suárez-Herrera, M. F.; Costa-Figueiredo, M.; Feliu, J. M. Voltammetry of Basal Plane Platinum Electrodes in Acetonitrile Electrolytes: Effect of the Presence of Water. *Langmuir* **2012**, *28* (11), 5286−5294.
(59) Foley, J. K.; Korzeniewski, C.; Pons, S. Anodic and Cathodic Reactions in Acetonitrile/Tetra-n-Butylammonium Tetrafluoroborate: An Electrochemical and Infrared Spectroelectrochemical Study. *Can. J. Chem.* **1988**, *66* (1), 201−206.
(60) Gunathunge, C. M.; Li, J.; Li, X.; Waegele, M. M. Surface-Adsorbed CO as an Infrared Probe of Electrocatalytic Interfaces. *ACS Catal.* **2020**, *10* (20), 11700−11711.

https://doi.org/10.1021/acs.jpcc.3c03257
J. Phys. Chem. C 2023, 127, 14518−14527